Thermal Issues in Micromachined Spiral Inductors for High-Power Applications

Huseyin Sagkol, *Student Member, IEEE*, Behzad Rejaei, and Joachim N. Burghartz, *Fellow, IEEE*

***Abstract*—An experimental study of the self-heating of micromachined spiral inductors operated under high-power conditions is presented. Typical suspended spiral coils are shown to develop highly elevated temperatures (up to several hundred degrees) under the flow of a moderate to high ($>$ 60 mA) dc current, which often applies to inductors in radio frequency power circuits. This can lead to the degradation of quality factor and even device failure. The role of various heat dissipation mechanisms relevant for a suspended coil is discussed and analyzed by means of experiments and thermal simulations. Possible solutions to the self-heating issue are discussed and experimentally demonstrated.**

***Index Terms*—Micromachining, microwave circuits, passives, self-heating, spiral inductor.**

I. Introduction

INDUCTORS are key components in low-noise amplifiers, oscillators, filters, and impedance matching networks implemented in radio frequency (RF) integrated circuits. Emphasis lies on integration in silicon (Si) technology, providing advantages in terms of reliability, cost, and integration density. The major drawback of Si-based inductors, however, is the high level of RF losses in the metal coil structure and in the conductive silicon substrate. These losses prevent, in general, from achieving high quality factors (Q) for spiral inductors on silicon.

In spite of the extensive efforts to tackle the substrate loss issue, the problem continues to be important and is thus being addressed in the semiconductor technology roadmap [1]. Solutions to the substrate loss include the use of high-resistivity Si (HRS) [2]–[4], thick dielectric layers [5]–[8], proton bombardment of Si [9], [10], and oxidized deep trenches [11], [12]. Although effective, such methods involve major modification of the core device integration process, leading to process incompatibility and, thus, considerably higher cost.

An alternative approach based on local removal of the Si substrate [13]–[15] has gained attention since it can be implemented by an add-on micromachining process, leaving the core integration process unaffected [16]. Moreover, the comparison of the process modifications mentioned (Fig. 1) shows, by far, the best results for Si micromachining in terms of the maximum Q obtained. However, while suspension of inductors by micromachining yields significantly higher Q's in low power RF circuits [13]–[16], its application to high-power circuits like power amplifiers (PAs) is still an unexplored area. As the integration of PAs is considered a viable direction by industry [1], it is important to study the compatibility of suspended inductors with power circuit integration.

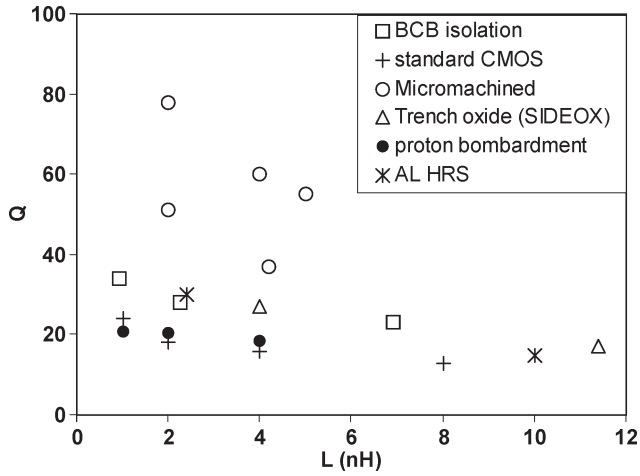

Fig. 1. Inductance (L) and quality factor (Q) values for different technology options for the fabrication of integrated inductors. Data were taken from [2]–[19]. Hollow markers indicate the inductors that are prone to self-heating.

The most serious problem faced by suspended inductors in PA applications is self-heating due to the flow of a high dc or RF current [20]. The lack of an effective heat dissipation path, caused by the removal of the Si underneath the coil, leads to elevated temperatures inside the current carrying coil. This, in turn, causes performance degradation and raises concerns about reliability [21]–[26].

The research presented in this paper is dedicated to an experimental study, supported by modeling and simulations, of the self-heating of suspended spiral inductors under high-power conditions. We demonstrate that the average coil temperature may rise to several hundred degrees under the application of moderate to high currents ($>$ 60 mA). In some cases, the local temperature of the coil can even be high enough to melt the metal lines, leading to device failure. We show that conduction through the coil's metal is the most effective heat dissipation path for a suspended inductor, although it does not prevent from self-heating if the metal lines have normal thickness. We shall also pay attention to the role of the underlying membrane and the surrounding air. Simulation based on mapping the thermal problem onto a dc-conduction model will be employed

Manuscript received January 15, 2008; revised June 20, 2008. Current version published October 30, 2008. The review of this paper was arranged by Editor C. Nguyen.

H. Sagkol and B. Rejaei are with the Electrical Engineering, Mathematics and Computer Science Department, Delft University of Technology, 2600 Delft, The Netherlands (e-mail: h.sagkol@ewi.tudelft.nl; b.rejaei@ewi.tudelft.nl).

J. N. Burghartz is with the Institute for Microelectronics Stuttgart, 70569 Stuttgart, Germany, and also with the Institute of Nano and Microelectronic System, University of Stuttgart, 70569 Stuttgart, Germany (e-mail: burgh@ims-chips.de).

Digital Object Identifier 10.1109/TED.2008.2005127

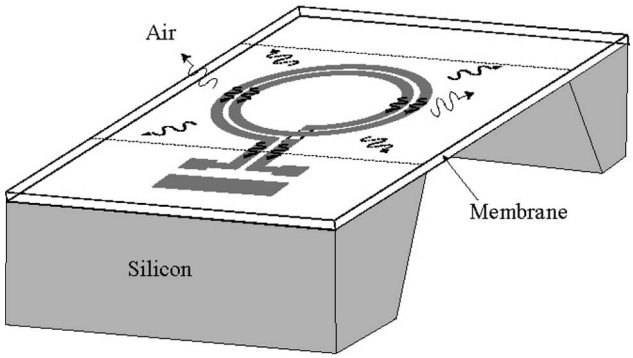

Fig. 2. Three-dimensional image of a suspended inductor. The heat generated inside the coil is carried away through the coil conductor and the dielectric membrane to reach the silicon substrate. The surrounding air provides an additional route for the transfer of the excessive heat.

to gain better understanding of the experimental data, as well as various heat dissipation mechanisms. Finally, we discuss possible solutions to achieve both a high Q and suppression of self-heating.

II. Self Heating of Suspended Inductors

Under high-power conditions, the heat generated inside a conventional integrated spiral inductor is carried away through the underlying bulk Si, which has an excellent thermal conductivity. In contrast, a suspended inductor (Fig. 2) has to suffice with alternate paths for the heat flow, such as through the metal of the spiral coil, the underlying dielectric membrane, and by conduction and convection through the air. In comparison, heat dissipation through the conductor is expected to be dominant due to very high thermal conductivity of metal. The internally generated heat will then flow through the coil outward to the leads that connect to the circuitry on the silicon substrate. The bulk silicon will thus act as a heat sink and set a reference ambient temperature.

Heat conduction through the dielectric membrane, in the case that such a membrane structure is used, is less significant since the thermal conductivity of commonly used materials (SiO_2 and Si_3N_4) is typically two orders of magnitude lower than that of metals. Moreover, the membrane is usually thin (several micrometers). Nevertheless, the membrane's contribution to heat dissipation may not be fully negligible as the thermal path through the metal coil is much longer in comparison. Finally, heat can be dissipated through air, which, in spite of its very low thermal conductivity (one order of magnitude smaller than that of typical membrane dielectrics), has to be considered since it offers conduction paths through the whole coil surface.

In terms of heat transfer efficiency, the paths outlined earlier can by no means substitute for the heat transfer through the bulk silicon, as available to conventional integrated inductors. Consequently, suspended inductors operating under high-power conditions become prone to excessive self-heating effects, which degrade their performance and reliability. In order to gain more insight into this problem, we fabricated various suspended circular inductors with the geometrical parameters, i.e., number of turns (N), radius (r), linewidth (w), and spacing (s), listed in Table I. The devices were built by using a Si micromachining postprocess module added to an in-house standard active device process that has two aluminum (Al) metal layers with thicknesses of 0.8 μm at M1 and 3 μm at M2 levels. The M1 layer is used as the underpass for the inductors, and M2 is exploited for the spiral coil itself. There is a 0.8-μm-thick PECVD SiO_2 layer in between the M1 and M2 layers. The M1 layer rests on 3.2-μm SiO_2, which results in 4-μm total membrane thickness for the spiral. Several inductors are placed onto a strip, with the entire strip of Si substrate being etched away by using deep reactive ion etching.

The high-frequency parameters (inductance and quality factor) of the coils were extracted from S-parameter data obtained with an HP 8510 network analyzer equipped with bias-T's to supply the dc bias current. The high-power conditions were emulated by subjecting the inductors to a constant dc bias current between 0 and 100 mA while measuring their resistance using a voltmeter. The resulting dc power applied to the devices was considered as the self-heating power emulating the case of an inductor that has only high RF power passing through. Note that, although in the RF case current distribution—and, thus, heat generation—in the cross section of the coil is nonuniform due to skin depth and proximity effects, the high thermal conductivity of metal makes the heat distribution in the cross section uniform, hence making it the same with the dc case. Since there is no added value in experimenting with RF load currents, we limited ourselves to the dc case, which is much easier to handle.

Table I shows the increase in the average temperature $T_{\rm av}$ of the suspended coils under different bias currents $(I_{\rm dc})$. For each bias applied, $T_{\rm av}$ was determined by measuring the dc resistance $R_{\rm dc}$ of the inductor and by calculating the average resistivity $\rho_{\rm av}$ of the conductor from the relation

$$\rho_{\rm av}(I_{\rm dc}) = \frac{R_{\rm dc}(I_{\rm dc})}{R_{\rm dc}(0)}\rho_0. \tag{1}$$

Here, ρ_0 denotes the electrical resistivity of Al without the applied bias, i.e., at room temperature. The average temperature of the coil was then evaluated by using

$$T_{\rm av}(I_{\rm dc}) = T_0 + \left(\rho_{\rm av}(I_{\rm dc}) - \rho_0\right)/(\alpha\rho_0) \tag{2}$$

where α is the temperature coefficient of resistance of the metal $(\alpha = 0.0043\ 1/^\circ\mathrm{C})$.

The data in Table I show a dramatic increase in the average temperature (up to several hundred degrees) for some of the inductors under bias currents higher than 60 mA. One should bear in mind, however, that inductors with a different series resistance do not dissipate the same amount of power $(P = R_{\rm dc}I_{\rm dc}^2)$ for equal bias currents. A more appropriate figure of merit for comparison of the thermal behavior of inductors is, therefore, the increase in average temperature per unit of dissipated power (ζ). The corresponding data are shown as the last column in Table I.

The rise in inductor temperature as a result of applied bias is governed by the tradeoff between local heating by the dissipation of electric power and the transfer of the heat to the ambient environment. Given the expected dominance of heat

TABLE I
INDUCTANCE (L), NUMBER OF TURNS (N), LINE WIDTH (w), SPACING (s), RADIUS (r), AND TOTAL METAL LENGTH (l) OF SUSPENDED CIRCULAR SPIRAL INDUCTORS USED IN THE EXPERIMENTS. FOR EACH COIL, THE INCREASE IN AVERAGE TEMPERATURE WITH RESPECT TO THE ROOM TEMPERATURE ($\Delta T_{\rm av}$) WAS MEASURED AS A FUNCTION OF AN APPLIED DC BIAS CURRENT. THE LAST COLUMN PRESENTS THE CALCULATED TEMPERATURE INCREASE PER UNIT DISSIPATED POWER

Coil nr.	L (nH)		Dimensions (μm)				ΔT_{av} (°C) for different bias currents					ζ (°C/mW)
		N	w	s	r	l	20 mA	40 mA	60 mA	80 mA	100 mA	
1	1	2	6	3	80	854.1	5.6	22.9	57.5	121.4	256.7	6.392
2	1	2	6.8	13.8	100	955.3	6.5	25.8	60.4	122.3	244.9	7.2
3	1	2	11.8	3.3	100	992.2	1.9	8.8	21.5	38.2	65.5	5.115
4	1	2	16.4	7.6	120	1102.5	1.8	6.8	19.4	33.0	51.9	5.32
5	1	2	6.5	28.9	120	1021.1	5.1	25.4	66.5	147.7	346.6	6.838
6	1	2	14.2	35.8	150	1167.1	4.2	8.1	22.3	42.1	73.1	5.56
7	1	2	23.8	14.9	150	1249	2.1	3.9	14.6	24.7	39.0	4.95
8	5	4	23.1	3	200	3421	2.8	10.9	28.5	55.2	98.3	4.038
9	5	3	25.3	5.8	250	3593.6	5.9	10.0	27.4	51.7	89.5	3.98
10	5	3	35.3	10.7	300	4019.5	1.0	11.0	21.3	38.9	63.2	3.65
11	5	3	15.6	4.1	200	3062	4.9	20.2	46.0	88.9	162.3	4.556
12	5	3	17.4	21.1	250	3460.4	4.7	20.2	49.3	98.5	182.5	4.759
13	10	5	15.00	3	200	4631.7	5.5	28.7	77.8	175.4	464.6	4.446
14	10	4	18.6	3	250	4961.8	4.1	20.1	51.6	106.5	206.0	3.785
15	10	5	21.6	5.2	250	5407.1	5.6	22.2	53.8	109.9	210.4	4.16
16	10	4	23.5	10.9	300	5517.7	4.7	21.2	49.5	100.3	187.1	4.078
17	10	4	26.4	4.1	300	5672.1	3.3	16.3	41.0	80.8	146.1	3.818
18	10	4	34.2	7.5	350	6267.4	2.8	11.9	30.2	58.9	102.5	3.38

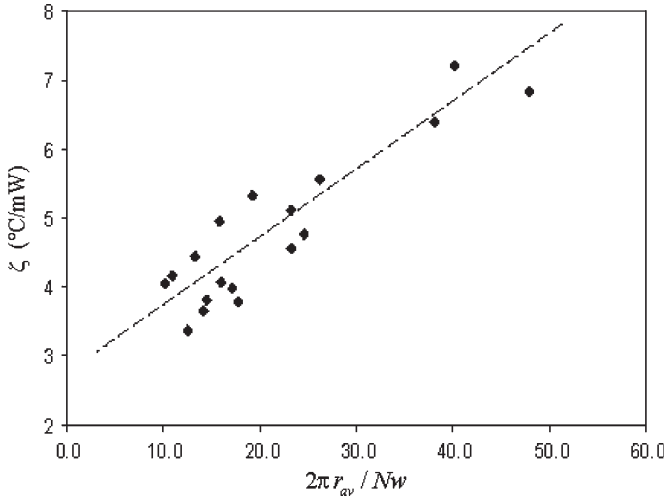

Fig. 3. Average temperature increase per dissipated power (ζ) versus the ratio between the average circumference of the coil ($2\pi r_{\rm av}$) and the total metal width (Nw) $\cdot$ $r_{\rm av}$ equals the average of the outer and inner radii of the coil. The correlation observed indicates that, from a thermal perspective, a suspended coil behaves as a single-turn inductor with the length $2\pi r_{\rm av}$ and the width Nw.

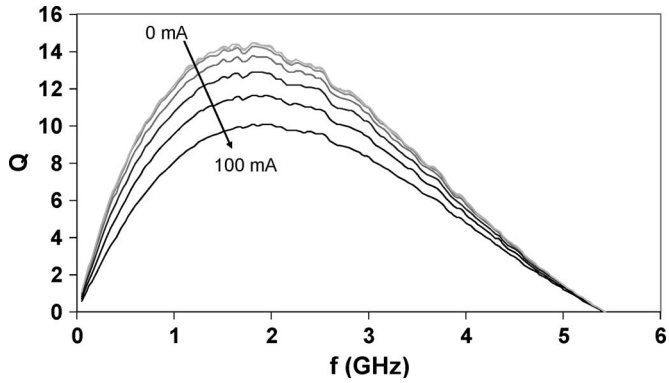

Fig. 4. Quality factor (Q) of a 10-nH suspended spiral inductor (coil nr. 15 in Table I) as a function of frequency for different bias currents. The data are extracted from the S-parameter measurements performed, by means of an HP 8510 network analyzer, under five different dc bias conditions. The rise in temperature caused by the dissipation of electric power leads to an increased series resistance and, thus, a reduced Q.

transfer through the metal coil, one would expect ζ to be mainly a function of its thermal resistance. The latter is proportional to l/w, where l is the total length of the coil. Close inspection of the results, however, reveals no clear correlation between ζ and l/w values. Instead, a correlation was found between ζ and $2\pi\ r_{\rm av}/Nw$, where $r_{\rm av}$ is the average radius of the coil (Fig. 3). Apparently, the different turns of the coil behave thermally as a single winding with the length $2\pi\ r_{\rm av}$ and the width Nw. This implies that the windings are in local thermal equilibrium with each other, so that neighboring points on different windings are essentially at the same temperature.

To understand this phenomenon, we should recall that the spacing (s) between the windings of the coil is small compared to their circumference. Despite its low thermal conductivity, the membrane can then act as an efficient lateral heat path locally shunting the neighboring turns. Hence, although heat transfer still takes place mainly through the metal, the inductor thermally behaves as a single-turn coil with an effective width given by the total width of the windings. These observations will be numerically verified in Section IV.

III. DETRIMENTAL EFFECTS OF SELF HEATING

The self-heating of suspended coils degrades their RF performance by lowering their quality factor (Q) [20]. Fig. 4 shows

TABLE II
GEOMETRICAL PARAMETERS OF THE SUSPENDED INDUCTORS WHICH FAILED DURING THE EXPERIMENTS, TOGETHER WITH THE INCREASE IN THEIR AVERAGE TEMPERATURE PRIOR TO THE FAILURE. THE LAST COLUMN SHOWS THE COMPUTED (SEE SECTION IV) MAXIMUM TEMPERATURE INSIDE THE COIL METAL AT THE BREAKDOWN BIAS CURRENT. SINCE THE CURRENT WAS INCREASED IN STEPS OF 20 mA, THE REPORTED VALUES OF THE BREAKDOWN CURRENT OVERESTIMATE THE ACTUAL ONES. AS A RESULT, THE COMPUTED MAXIMUM TEMPERATURES OVERESTIMATE THE TRUE VALUES

Coil nr.		Dimensions (μm)			ΔT_{av} (°C) for different bias currents (mA)					Peak ΔT (°C)
	N	w	s	r	20	40	60	80	100	
19	4	10.04	24.34	300	15	71	205	x	x	782
20	3	10.32	17.8	350	15	71	205	x	x	782
21	3	5.18	14.11	200	27	156	x	x	x	811
22	3	13.21	11.12	350	3	32	91	198	x	597
23	4	13.61	17.78	300	11	46	124	301	x	1072
24	3	6.79	10.74	200	14	77	253	x	x	1070

the Q of a suspended inductor as a function of frequency for different bias currents. Up to 30% reduction of the maximum Q value can be observed. This can be attributed to temperature-induced increase of the series resistance of the coil.

A more crucial problem, however, involves the reliability issue caused by excessive heating. While the values given in Table I represent average coil temperatures, the local temperature of the metal may rise up to much higher values. This may result in device failure due to local breakdown of the coil metal by electromigration effects, stress-induced cracks, or even melting. To experimentally study these effects, we monitored the dc resistance of inductors as the dc bias current was increased from 0 to 100 mA in steps of 20 mA. The current was then reduced back to 0 mA in order to verify if a permanent damage occurred to the coils after the current cycle. During the measurement, it was observed under a microscope that some of the inductors (listed in Table II) were burned, resulting in a flash of light. Later, those inductors were examined by using a scanning electron micrograph (SEM). One sample SEM is shown in Fig. 5, where it is possible to observe small dots adjacent to the metal coil tracks. These little spheres are indeed molten Al, later solidified, which takes spherical form due to surface tension. This observation suggests the fact that Al tracks melt during breakdown due to excessive temperature.

Fig. 5 clearly shows that metal damage simultaneously occurs on several points far away from the coil terminals (although, most likely, complete breakdown occurs at only one of those points, cutting the current path). Evidently, since the coil interconnects partially lie on the silicon substrate (acting as a heat sink at ambient temperature), high temperatures can only develop at sufficient distance from those points. Furthermore, note that, although the damaged points lie on different windings, they are closely neighbored. This indirectly verifies our previously made hypothesis that adjacent points on different windings essentially have the same temperature.

To gain more insight into the mechanism of device failure, we carried out simulations (see next section) to compute the maximum local temperature inside the coil metal at the breakdown bias (Table II). Although the values obtained overestimate

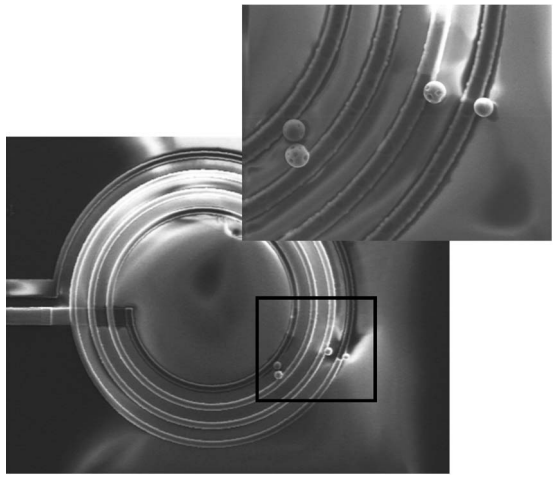

Fig. 5. SEM image of a spiral inductor that has failed due to excessive self-heating. Little spheres are molten aluminum metal of the spiral tracks that later solidifies. It is also possible to observe the voids in the metal tracks in the zoomed picture.

the actual ones (see the caption of Table II), they indicate that the local temperature inside the coils can easily rise to the melting point of Al (660 °C). This result explains the molten Al particle observed under the microscope. However, one should bear in mind that electromigration effects and stress-induced cracks in the metal due to warpage of the membrane can potentially accelerate the melting process. In particular, the stress-induced cracks can locally narrow down the current carrying wires, leading to increased local resistance and, therefore, heat generation. However, those effects could not be verified by our experiments.

IV. COMPUTATIONAL MODEL

In order to quantitatively analyze the self-heating of suspended inductors and to support the experimental results obtained, we carried out simulations by mapping the thermal problem onto a dc-conduction problem. The transfer of heat inside any medium is governed by the Fourier's law of conduction

$$\boldsymbol{q}(\boldsymbol{r}) = -k\nabla T(\boldsymbol{r}) \tag{3}$$

where $\boldsymbol{q}$ is the heat flux density vector, $\boldsymbol{r} = (x, y, z)$, k is the thermal conductivity of the medium, $\nabla = (\partial_x, \partial_y, \partial_z)$, and T is the local temperature. In the steady state, the aforementioned equation is supplemented by

$$\nabla \cdot \boldsymbol{q}(\boldsymbol{r}) = p(\boldsymbol{r}) \tag{4}$$

where p denotes the time rate of heat generation per unit volume.

Equations (3) and (4) are identical to those governing the distribution of electrical current in conducting media with $\boldsymbol{q}$, T, k, and p replaced by the electric current density, potential, conductivity, and time rate of electric charge generated per unit volume, respectively. The problem can thus be analyzed by using any electromagnetic simulation package, provided that special measures are taken to incorporate local heat generation (or charge generation in the analogous electric case) by the dissipation of electric power. In a simulation program, this

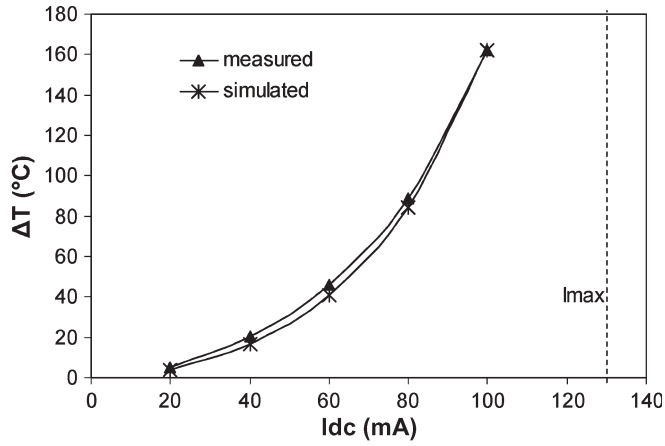

(a)

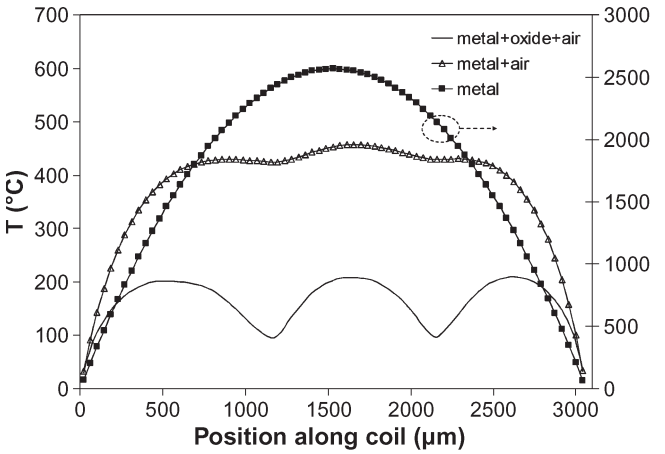

(b)

Fig. 6. (a) Simulated versus measured average temperature of a three-turn suspended inductor (coil nr. 11 in Table I) as a function of the applied bias current. $I_{\max}$ line indicates the maximum applicable current before the destruction of the coil. (b) (Solid line) Simulation results for temperature as a function of position along the same coil for an applied bias of 100 mA. Valleys in the graph correspond to regions close to the contact points of the spiral. The curve marked with squares shows the results obtained for the metal alone, i.e., neglecting the thermal effect of air and the oxide membrane. In this case, extremely high temperatures ($>$ 2000 °C!) are reached at the center of the coil. The line marked with triangles shows the results obtained in the presence of air but without the membrane.

can be achieved by dividing the coil into a number of small segments along its length and assigning a separate terminal (port) to each segment. The local generation of heat can then be approximately taken into account by considering the total heat generated inside each division

$$\Delta Q = \int_{\Delta V} p(\boldsymbol{r})\, dV = I_{\rm dc}^2 \Delta R \tag{5}$$

as a current fed through the corresponding port. In the aforementioned equation, ΔV and ΔR denote the volume and electric resistance, respectively, of a segment.

Using this method in combination with Agilent's software tool ADS, we simulated the temperature distribution inside the suspended coils. While we could not experimentally verify the local temperatures, good agreement (7%–15% error) was found between the calculated and measured average coil temperatures. Fig. 6(a) shows these values for a 5-nH inductor (coil nr. 11 in Table I) as a function of the applied bias. The calculated temperature (T) distribution along the same coil is shown in Fig. 6(b) (solid line) for a bias current of 100 mA. The start and end points of the curve correspond to the coil terminals that are at ambient (room) temperature. Notice the nearly periodic dependence of T on the location within the coil. This clearly suggests local thermal equilibrium between the windings. If simulations are performed for the metal alone, no periodic dependence is observed [see Fig. 6(b)]. Instead, the temperature along the coil exhibits the usual parabolic behavior in a metal wire and reaches extremely high values at the center of the coil. Hence, the membrane is crucial for preventing excessive self-heating not necessarily because of its ability to conduct the heat away from the coil but to thermally shunt the windings, thus decreasing the effective length and increasing the effective width of the metal with respect to thermal conduction. Interestingly, the surrounding air can also contribute to this effect. Simulations performed without the membrane but including conduction through air show a considerable lowering of the coil temperature with respect to those obtained for the metallic coil alone [see Fig. 6(b)]. They also show a slight periodicity similar to the effect of the membrane.

TABLE III
HEAT DISSIPATION PERCENTAGES FOR A NUMBER OF SUSPENDED INDUCTORS. METAL DENOTES THE DISSIPATION THROUGH THE METAL TRACKS, OXIDE IS FOR HEAT DISSIPATION THROUGH THE 4-μm-THICK SILICON DIOXIDE MEMBRANE, AND AIR IS FOR THE CONDUCTION THROUGH AIR

Coil nr.	Metal (%)	Oxide (%)	Air (%)
1	76.9	14.9	8.2
2	80.3	12.6	7.1
8	74.5	15.5	10
11	63.6	22.5	13.9
13	72.8	13	14.2

Finally, in Table III, we have summarized the percentage of heat dissipation through different routes available to a suspended inductor. For typical coils built on a 4-μm-thick silicon dioxide membrane, about 60%–80% of the heat is carried away through the metal, 12%–20% is dissipated through the membrane, and 7%–15% is conducted through the air.

V. THERMAL MANAGEMENT IN SUSPENDED COILS

The results presented in the previous section show that the most effective way to prevent excessive heating of suspended coils in power applications is to increase the efficiency of heat transfer through the coil metal itself. This can be achieved by increasing the width of the metal turns. Yet, this solution is not always in support of RF performance, as it increases the parasitic interwinding capacitance for a given metal pitch, leading to a reduction of the self-resonance frequency of the device [27]. Instead, increasing the metal thickness and/or using metals with a high thermal (and thus electrical) conductivity such as copper (Cu) is more favorable. To study this effect, we built suspended inductors from 13-μm-thick electroplated Cu using a process described in [28]–[30]. Fig. 7 shows the comparison of suspended Al- and Cu-based inductors in terms of temperature increase as a function of applied current. The Cu-based coil apparently leads to a far more effective heat

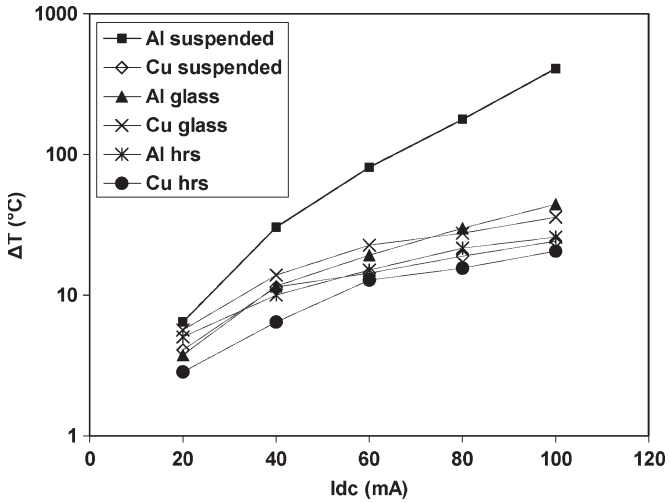

Fig. 7. Increase in average temperature as a function of the applied current for a 5-nH inductor (coil nr. 9 in Table I) fabricated using different technologies. All Al inductors have a thickness of 3 μm, and all Cu inductors have a thickness of 13 μm. The suspended Cu-based coil shows a tenfold reduction of average temperature compared to the suspended Al-based device. The same coil built on an HRS substrate shows almost no self-heating effect.

removal than its Al-based counterpart. Moreover, for a given current, the amount of electric power dissipated in the Cu-based inductor is less due to its smaller series resistance. Overall, the result is an almost tenfold reduction of average temperature.

In power applications, where thick highly conductive metal layers are not readily available, one should consider increasing the heat transfer efficiency of the nonmetallic thermal paths described earlier. Possible solutions are to increase the membrane thickness (to several tens of micrometers) or to cover the coil by a thermally conductive, but electrically insulating, layer such as the encapsulating plastic packaging (heat shunt). The first option, however, is not technologically viable due to the excessive stress build up in the substrate. The second solution, on the other hand, adds to the complexity of the fabrication process. Moreover, the electrical properties (e.g., dielectric constant and loss) of such a heat shunt affect the device performance and should thus be applied with caution. The best alternative in this case, in fact, is to use nonsuspended coils. In order to provide a coil structure that features both a high Q and a high thermal conductivity to the substrate, one should consider fabricating coils on substrates with low RF loss yet good thermal conductivity, such as HRS [2]–[4]. The comparison of experimental data obtained (see Fig. 7) shows that HRS-based inductors suffer the least from self-heating effects. Evidently, the effectiveness of an HRS substrate as a heat conductor cannot be matched even by very thick Cu coils.

VI. Conclusion

We have presented a study of self-heating of suspended spiral inductors under high-power operating conditions. Experimental data obtained from typical spiral inductors show that the average device temperature may rise to several hundred degrees for moderate to high dc (or RF) currents (above 60 mA) applied. This leads to a degradation of the RF performance of the coils (lower quality factor) and, in some cases, even to the catastrophic failure of the device.

The excessive self-heating of suspended inductors is caused by the limited efficiency of the thermal dissipation paths available. Among those paths, heat conduction through the coil metal is the most effective. Nevertheless, the underlying membrane and the surrounding air are crucial for preventing extreme self-heating not necessarily because of their efficiency in dissipating the heat but since they thermally shunt the metallic windings. This hypothesis was supported by simulations based on mapping the thermal problem onto a dc-conduction problem. The results were in good agreement with the experiments.

A remedy to the self-heating of suspended coil is offered by deploying thick highly conductive metals. Experimental data obtained from coils built from 13-μm-thick electroplated Cu lines prove the absence of excessive heating even for very high values of dc supply currents. In the absence of a thick metal, the best alternative is to resort to conventional coils built on a low-loss, but thermally conductive, substrate such as HRS.

Acknowledgment

The authors would like to thank A. Akhnoukh, H. Schellevis, and P. M. Sarro from the Delft Institute of Microsystems and Nanoelectronics, Delft University of Technology, The Netherlands, for the support in high-frequency device characterization and silicon processing.

References

[1] *International Technology Roadmap for Semiconductors*. 2005 edition.
[2] B. Rong, J. N. Burghartz, L. K. Nanver, B. Rejaei, and M. van der Zwan, "Surface-passivated high-resistivity silicon substrates for RFICs," *IEEE Electron Device Lett.*, vol. 25, no. 4, pp. 176–178, Apr. 2004.
[3] J. N. Burghartz, D. C. Edelstein, K. A. Jenkiin, and Y. H. Kwark, "Spiral inductors and transmission lines in silicon technology using copper-damascene interconnects and low-loss substrates," *IEEE Trans. Microw. Theory Tech.*, vol. 45, no. 10, pp. 1961–1968, Oct. 1997.
[4] A. C. Reyes, S. M. El-Ghazaly, S. J. Dorn, M. Dydyk, D. K. Schroder, and H. Patterson, "Coplanar waveguides and microwave inductors on silicon substrates," *IEEE Trans. Microw. Theory Tech.*, vol. 43, no. 9, pp. 2016–2022, Sep. 1995.
[5] G. J. Carchon, W. De Raedt, and E. Beyne, "Wafer-level packaging technology for high-Q on-chip inductors and transmission lines," *IEEE Trans. Microw. Theory Tech.*, vol. 52, no. 4, pp. 1244–1251, Apr. 2004.
[6] B. K. Kim, B. K. Ko, K. Lee, J. W. Jeong, K. S. Lee, and S. C. Kim, "Monolithic planar RF inductor and waveguide structures on silicon with performance comparable to those in GaAs MMIC," in *IEDM Tech. Dig.*, 1995, pp. 717–720.
[7] D. C. Laney, L. E. Larson, P. Chan, J. Malinowski, D. Harame, S. Subbanna, R. Volant, and M. Case, "Microwave transformers, inductors, and transmission lines implemented in an Si/SiGe HBT process," *IEEE Trans. Microw. Theory Tech.*, vol. 49, no. 8, pp. 1507–1510, Aug. 2001.
[8] X. Huo, K. J. Chen, and P. C. H. Chan, "Silicon-based high-Q inductors incorporating electroplated copper and low-K BCB dielectric," *IEEE Electron Device Lett.*, vol. 23, no. 9, pp. 520–522, Sep. 2002.
[9] K. T. Chan, C. H. Huang, A. Chin, M. F. Li, D. L. Kwong, S. P. McAlister, D. S. Duh, and W. J. Lin, "Large Q-factor improvement for spiral inductors on silicon using proton implantation," *IEEE Microw. Wireless Compon. Lett.*, vol. 13, no. 11, pp. 460–462, Nov. 2003.
[10] A. Chin, K. T. Chan, C. H. Huang, C. Chen, V. Liang, J. K. Chen, S. C. Chien, S. W. Sun, D. S. Duh, W. J. Lin, C. Zhu, M. F. Li, S. P. McAlister, and D. L. Kwong, "RF passive devices on Si with excellent performance close to ideal devices designed by electro-magnetic simulation," in *IEDM Tech. Dig.*, 2003, pp. 15.5.1–15.5.4.
[11] M. Raieszadeh, P. Monajemi, S. W. Yoon, J. Laskar, and F. Ayazi, "High-Q integrated inductors on trenched silicon islands," in *Proc. IEEE Int. Conf. Micro Electro Mech. Syst.*, 2005, pp. 199–202.

[12] J. Miao and J. Sun, "Integrated RF MEMS inductors on thick silicon oxide layers fabricated using SIDeox process," in *Proc. Int. Conf. Solid State Integr. Circuits Technol.*, 2004, pp. 1683–1686.
[13] J. Y. C. Chang, A. A. Abidi, and M. Gaitan, "Large suspended inductors on silicon and their use in a 2-μm CMOS RF amplifier," *IEEE Electron Device Lett.*, vol. 14, no. 5, pp. 246–248, May 1993.
[14] J. W. Lin, C. C. Chen, and Y. T. Cheng, "A robust high-Q micromachined RF inductor for RFIC applications," *IEEE Trans. Electron Devices*, vol. 52, no. 7, pp. 1489–1496, Jul. 2005.
[15] T. Wang, Y. S. Lin, and S. S. Lu, "An ultralow-loss and broadband micromachined RF Inductor for RFIC input-matching applications," *IEEE Trans. Electron Devices*, vol. 53, no. 3, pp. 568–570, Mar. 2006.
[16] J. N. Burghartz, M. Soyuer, K. A. Jenkins, Y. H. Kwark, S. Ponnapalli, J. F. Ewen, and W. E. Pence, "Opportunities for standard silicon technology in RF & microwave applications," in *Proc. ESSDERC*, 1995, pp. 363–367.
[17] Y. S. Choi and J. B. Yoon, "Experimental analysis of the effect of metal thickness on the quality factor in integrated spiral inductors for RF ICs," *IEEE Electron Device Lett.*, vol. 25, no. 2, pp. 76–79, Feb. 2004.
[18] X. N. Wang, X. L. Zhao, Y. Zhou, X. H. Dai, and B. C. Cai, "Fabrication and performance of a novel suspended RF spiral inductor," *IEEE Trans. Electron Devices*, vol. 51, no. 5, pp. 814–816, May 2004.
[19] D. Peroulis, S. Mohammadi, and L. P. B. Katehi, "High-Q integrated passive elements for high frequency applications," in *Proc. Top. Meeting Silicon Monolithic Integr. Circuits RF Syst.*, 2004, pp. 25–28.
[20] H. Sagkol, S. Sinaga, J. N. Burghartz, B. Rejaei, and A. Akhnoukh, "Thermal effects in suspended RF spiral inductors," *IEEE Electron Device Lett.*, vol. 26, no. 8, pp. 541–543, Aug. 2005.
[21] K. Kang, L. W. Li, S. Zouhdi, J. Shi, and W. Y. Yin, "Electromagnetic-thermal analysis for inductances and eddy current losses of on-chip spiral inductors on lossy silicon substrate," in *Proc. Eur. Microw. Integr. Circuits Conf.*, Sep. 2006, pp. 13–16.
[22] M. C. Hsieh, Y. K. Fang, C. H. Chen, S. M. Chen, and W. K. Yeh, "Design and fabrication of deep submicron CMOS technology compatible suspended high-Q spiral inductors," *IEEE Trans. Electron Devices*, vol. 51, no. 3, pp. 324–331, Mar. 2004.
[23] L. Krishnamurthy, V. T. Vo, and A. A. Rezazadeh, "Thermal characterization of compact inductors and capacitors for 3D MMICs," in *Proc. 36th Eur. Microw. Conf.*, 2006, pp. 52–55.
[24] H. W. Chiu, Y. S. Lin, K. Liu, and S. S. Lu, "Temperature and substrate effects in monolithic RF inductors on silicon with 6 μm-thick top metal for RFIC applications," *IEEE Trans. Semicond. Manuf.*, vol. 19, no. 3, pp. 316–330, Aug. 2006.
[25] R. Groves, D. L. Harame, and D. Jadus, "Temperature dependence of Q and inductance in spiral inductors fabricated in a silicon–germanium/BiCMOS technology," *IEEE J. Solid State Circuits*, vol. 32, no. 9, pp. 1455–1459, Sep. 1997.
[26] Y. S. Lin and S. H. Wu, "Temperature and substrate thickness dependence of Q and NF in broadband spiral inductors for CMOS RF MEMSOC applications," in *Proc. 4th ICMMT*, Aug. 2004, pp. 602–605.
[27] J. N. Burghartz and B. Rejaei, "On the design of RF spiral inductors on silicon," *IEEE Trans. Electron Devices*, vol. 50, no. 3, pp. 718–729, Mar. 2003.
[28] B. Rejaei, J. N. Burghartz, and H. Schellevis, "Saddle add-on metallisation (SAM) for RF inductor implementation in standard IC interconnects," in *IEDM Tech. Dig.*, 2002, pp. 467–470.
[29] J. N. Burghartz, B. Rejaei, and H. Schellevis, "Saddle add-on metallization for RF-IC technology," *IEEE Trans. Electron Devices*, vol. 51, no. 3, pp. 460–466, Mar. 2004.
[30] H. Sagkol, B. Rejaei, and J. N. Burghartz, "High-Q saddle-add-on metallization (SAM) inductors on HRS substrates," in *Proc. Top. Meeting Silicon Monolithic Integr. Circuits RF Syst. Dig. Papers*, Jan. 2006, pp. 245–247.

Huseyin Sagkol (S'01) received the B.Sc. and M.Sc. degrees in electrical engineering form the Middle East Technical University, Ankara, Turkey, in 1999 and 2002, respectively. He is currently working toward the Ph.D. degree in the Electrical Engineering, Mathematics and Computer Science Department, Delft University of Technology, Delft, The Netherlands.

His research interests are micromachining process development, integrated RF passive components, and microwave circuit design.

Behzad Rejaei received the M.Sc. degree in electrical engineering from the Delft University of Technology, Delft, The Netherlands, in 1990 and the Ph.D. degree in theoretical condensed matter physics from the University of Leiden, Leiden, The Netherlands, in 1994.

From 1995 to 1997, he was a member of the Physics faculty with Delft University of Technology, where he carried out research on mesoscopic charge-density-wave systems. Since 1997, he has been with the Electrical Engineering, Mathematics, and Computer Science Department, Delft University of Technology, where he is currently an Associate Professor. His research interests are in the areas of integrated passive components, high-frequency ferromagnetic devices, and artificial materials.

Joachim N. Burghartz (M'90–SM'92–F'02) was born in Aachen, Germany, in 1956. He received the M.S. (Dipl.Ing.) degree in electrical engineering from the RWTH, Aachen, in 1982 and the Ph.D. (Dr.-Ing.) degree electrical engineering from the University of Stuttgart, Stuttgart, Germany, in 1987.

From 1982 to 1987, he was a Research Assistant with the University of Stuttgart, Germany, where he developed sensors with integrated signal conversion with a special focus on magnetic-field sensors. From 1987 to 1998, he was with the IBM Thomas J. Watson Research Center, Yorktown Heights, NY. His earlier research work at IBM included device applications of selective epitaxial growth of silicon, Si and SiGe high-speed transistor design and integration processes, and deep submicrometer CMOS technology. He and his colleagues at IBM Research demonstrated the first SiGe bipolar technology setting the basis for IBM's SiGe commercialization. From 1994 to 1998, he was interested in the development of circuit building blocks for SiGe RF front-ends, with a special interest in the integration of high-quality passive components on silicon, and, in particular, the optimization of integrated spiral inductors. In 1998, he was a Full Professor with the Delft University of Technology (TU Delft), Delft, The Netherlands, where he was the Chair of the High-Frequency Technology and Components group. His research interests continued to be on silicon RF technology, ranging from investigations on materials to the design of RF circuit building blocks. Since 1995, he has been setting several milestones in the development of integrated spiral inductors for high-frequency applications. From March 2001 to September 2005, he was the Scientific Director of the Delft Institute of Microelectronics and Submicrometer Technology. Since October 1, 2005, he has been the Director and Chairman of the board of the Institute for Microelectronics Stuttgart and a Full Professor with the University of Stuttgart. Since March 1, 2006, he has also been the Head of the Institute of Nano and Microelectronic System (INES), University of Stuttgart. In Stuttgart, he is leading a research program that is focused on industrial contract research in the areas of silicon technologies, advanced lithography, CMOS imagers, ASIC design, and continued education. Recently, his special research interest is on a new manufacturing technology for ultrathin chips aimed at 3-D ICs, flexible and ultrasmall electronics, and other applications. He also continues to supervise several Ph.D. students at TU Delft working on projects related to RF silicon technology. He has published more than 250 reviewed articles, and he is the holder of 22 patents.